JMEPEG (2012) 21:2354–2362
DOI: 10.1007/s11665-012-0160-0

©ASM International
1059-9495/$19.00

Curcumin Derivatives as Green Corrosion Inhibitors for α-Brass in Nitric Acid Solution

A.S. Fouda and K.M. Elattar

(Submitted March 13, 2011; in revised form January 20, 2012)

1,7-*Bis*-(4-hydroxy-3-methoxy-phenyl)-hepta-1,6-diene-4-arylazo-3,5-dione I-V have been investigated as corrosion inhibitors for α-brass in 2 M nitric acid solution using weight-loss and galvanostatic polarization techniques. The efficiency of the inhibitors increases with the increase in the inhibitor concentration but decreases with a rise in temperature. The conjoint effect of the curcumin derivatives and KSCN has also been studied. The apparent activation energy (E_a*) and other thermodynamic parameters for the corrosion process have also been calculated. The galvanostatic polarization data indicated that the inhibitors were of mixed-type, but the cathode is more polarized than the anode. The slopes of the cathodic and anodic Tafel lines (b_c and b_a) are maintained approximately equal for various inhibitor concentrations. However, the value of the Tafel slopes increases together as inhibitor concentration increases. The adsorption of these compounds on α-brass surface has been found to obey the Frumkin's adsorption isotherm. The mechanism of inhibition was discussed in the light of the chemical structure of the undertaken inhibitors.

Keywords α-brass, corrosion inhibitors, curcumin derivatives, HNO_3, synergistic effect

1. Introduction

Copper and its alloys, because of their excellent resistance to corrosion in neutral aggressive media and their ease of processing, are widely used in industries, particularly as condensers and heat exchangers in power plants (Ref 1). Owing to the electro-dissolution of copper in chloride solutions, there is a growing interest in inhibitors, for the application of copper or its alloys in marine environments. *N*-heterocyclic compounds have been widely used as corrosion inhibitors (Ref 2). Among these, azoles (Ref 3-8), amines (Ref 9-15), amino acids (Ref 16, 17), and many others. The effect of some phthalimide derivatives on copper corrosion in 2 N HNO_3 was previously investigated (Ref 18). Protection efficiency of organic inhibitors is attributed mainly to the presence of a polar group acting as an active center for adsorption on the metallic surface (Ref 19). There are many different uses of curcumin compounds in medicinal chemistry (Ref 20, 21), which form complexes with different metals (Ref 22), but no previous study has reported the use of these curcumin compounds as corrosion inhibitors. The aim of the present investigation is to study the effect of some curcumin derivatives as corrosion inhibitors for α-brass in 2 M HNO_3. The present study was designed to investigate (i) corrosion inhibition of α-brass in nitric acid solutions by some curcumin derivatives using weight-loss and galvanostatic polarization techniques; (ii) the effect of substituted groups on the inhibition efficiency; and (iii) the effect of temperature on the corrosion rate to calculate some thermodynamic parameters related to the corrosion process.

A.S. Fouda and **K.M. Elattar**, Department of Chemistry, Faculty of Science, El-Mansoura University, El-Mansoura 35516, Egypt. Contact e-mails: asfouda@hotmail.com.

2. Experimental Method

2.1 Material

The experiments were performed with α-brass alloy (Cu37Zn) in this study. The inhibitors used in this study were selected from curcumin derivatives, the general structure formula of which is 1,7-*bis*-(4-hydroxy-3-methoxy-phenyl)-hepta-1,6-diene-4-arylazo-3,5-dione (I-V), and are represented as follows:

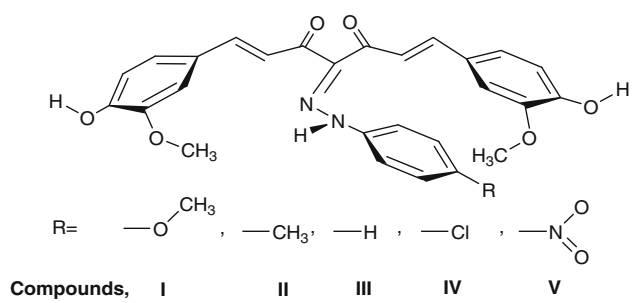

2.2 Preparation of Investigated Inhibitors

Curcumin derivatives were prepared by the general procedure as described in the next section.

2.2.1 Preparation of the Diazonium Salt. A solution of sodium nitrite (0.2 g in 2 mL water) was gradually added to a well-cooled solution of different aromatic amines (0.01 mol) in concentrated HCl (3.0 mL). The diazonium salt solution was added dropwise with continuous stirring to cold solution of curcumin in pyridine (20 mL). The reaction mixture was stirred

at 0-5 °C for 2 h and left to stand at room temperature. The solid product that obtained was filtered off, dried, and recrystallized from ethanol to give compounds (I-V) (Ref 23). From the infrared measurements of the prepared arylazo derivatives I-V, the presence of strong bands in the region 1550-1580 cm^{-1} indicating the (–N=N–) stretching frequency and the (NH) absorption was recorded at 3250 cm^{-1}, besides the (OH) stretching at 3400 cm^{-1}, Furthermore, the α,*b*-unsaturated carbonyl function appeared at 1690 cm^{-1}.

2.3 Solutions

100-mL stock solutions (10^{-3} M) of compounds (I-V) were prepared by dissolving an accurately weighed quantity of each material in an appropriate volume of absolute ethanol; then the required concentrations (1×10^{-6}-11×10^{-6} M) were prepared by dilution with bidistilled water.

Nitric acid solution was prepared by diluting the appropriate volume of the concentrated (70%) chemically pure acid, with bidistilled water, and its concentration was checked by standard solution of Na_2CO_3.

100-mL stock solution (1×10^{-2} M) of KSCN (BDH grade) was prepared by dissolving an accurately weighed quantity of each material in an appropriate volume of bidistilled water.

Two different techniques have been employed for studying the corrosion inhibition of α-brass by curcumin derivatives, these are (i) chemical technique (weight-loss method), and (ii) electrochemical technique (galvanostatic polarization method).

2.4 Quantum Chemical Calculations

All the quantum chemical calculations were performed with Material Studio semi-empirical program using PM3 method. The following quantum chemical indices were considered: The energy of the highest occupied molecular orbital (E_{HOMO}), energy of the lowest unoccupied molecular orbital (E_{LUMO}), $\Delta E = (E_{LUMO}) - (E_{HOMO})$, and dipole moment (μ).

2.5 Chemical Technique (Weight-Loss Method)

For weight-loss measurements, α-brass was used in the form of sheets having surface area of 1 cm^2. Before each experiment, the sheets were abraded, degreased with acetone, cleaned, and weighed. The weighed specimens were exposed in 100 mL of 2 M HNO_3 with and without the different concentrations of investigated curcumin compounds, for different periods. After exposure, the specimens were washed, dried, and weighed. Triplicate experiments have been performed to verify the reproducibility and consistency of the experimental data. The average weight loss at a certain time for each set of three samples was taken. The weight loss was recorded to the nearest 0.0001 g.

2.6 Electrochemical Technique

A typical three-compartment glass cell with capacity of 100 mL was used for the electrochemical tests. All the tests were performed at 30 ± 1 °C in non-deaerated solutions under unstirred conditions, using a thermostat. α-Brass with exposed area of 0.78 cm^2 cylindrical rod embedded in araldite with an exposed surface area of 0.78 cm^2 was used as working electrode, saturated calomel electrode (SCE) as reference electrode, and platinum foil as counter electrode. All the potentials are reported vs. SCE. Potentiodynamic polarization tests were conducted using potentiostatic/galvanostatic/Zera analyzer (Gamry PCI 300/4), and a personal computer with dc 105 software was used. Tafel polarization curves were obtained by changing the electrode potential automatically from −500 to −1000 mV_{SCE} at open circuit potential with a scan rate of 5 mV/s.

3. Results and Discussion

3.1 Weight-Loss Measurements

The inhibition efficiencies (%IE) and degree of surface coverage (θ) calculated for different concentrations of the various inhibitors by weight-loss method are reported in Table 1. From these results, it was found that, in general, as the concentration of the inhibitor was increased, the %IE and θ for all of the studied compounds increased. These data show that the greater the surface coverage of the adsorbed inhibitor, the higher the observed inhibition efficiency. The obtained weight loss-time curves are represented in Fig. 1 for inhibitor (I), the most effective one. Similar curves were obtained for other inhibitors (not shown). The inhibition efficiency of corrosion was found to be dependent on the inhibitor

Table 1 The effect of the presence of curcumin derivatives on the inhibition efficiency (%IE) and the surface coverage (θ) of α-brass in 2 M HNO_3 solution as obtained from weight-loss measurements

[Inhibitor], M	%IE	θ
2 M HNO_3 + compound I		
1×10^{-6}	16.7	0.167
3×10^{-6}	19.8	0.198
5×10^{-6}	23.7	0.237
7×10^{-6}	27.4	0.274
9×10^{-6}	32.0	0.320
11×10^{-6}	33.9	0.339
2 M HNO_3 + compound II		
1×10^{-6}	13.5	0.135
3×10^{-6}	17.2	0.172
5×10^{-6}	20.6	0.206
7×10^{-6}	23.3	0.233
9×10^{-6}	28.5	0.285
11×10^{-6}	31.6	0.316
2 M HNO_3 + compound III		
1×10^{-6}	11.4	0.114
3×10^{-6}	15.7	0.157
5×10^{-6}	18.2	0.182
7×10^{-6}	21.6	0.216
9×10^{-6}	26.8	0.268
11×10^{-6}	28.7	0.287
2 M HNO_3 + compound IV		
1×10^{-6}	9.3	0.093
3×10^{-6}	13.6	0.136
5×10^{-6}	16.2	0.162
7×10^{-6}	20.2	0.202
9×10^{-6}	24.6	0.246
11×10^{-6}	27.4	0.274
2 M HNO_3 + compound V		
1×10^{-6}	7.2	0.072
3×10^{-6}	12.3	0.123
5×10^{-6}	14.5	0.145
7×10^{-6}	17.9	0.179
9×10^{-6}	22.8	0.228
11×10^{-6}	26.6	0.266

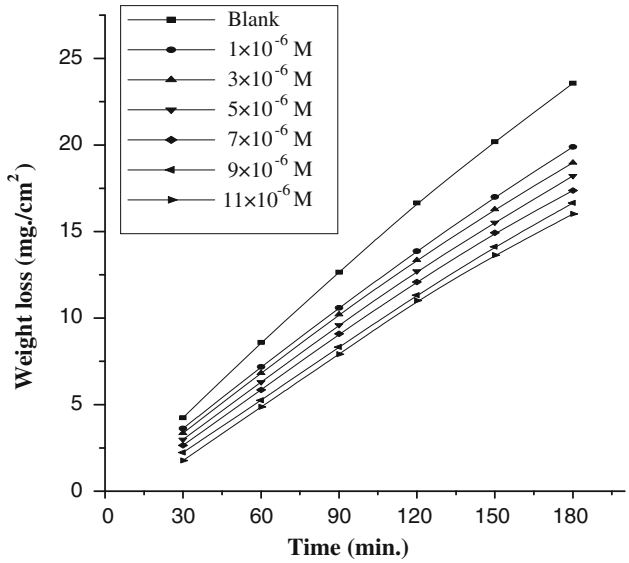

Fig. 1 Weight loss-time curves for α-brass dissolution in 2 M HNO_3 in the absence and presence of different concentrations of compound I at 30 °C

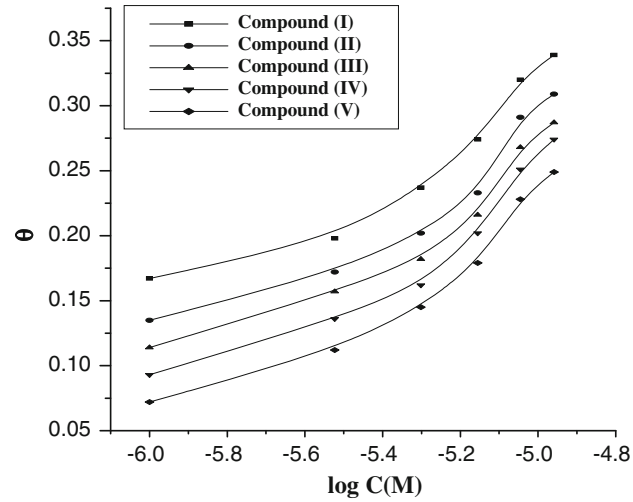

Fig. 2 θ vs. log C curves for α-brass dissolution in 2 M HNO_3 in the presence of different concentrations of all inhibitors from weight-loss measurements at 30 °C

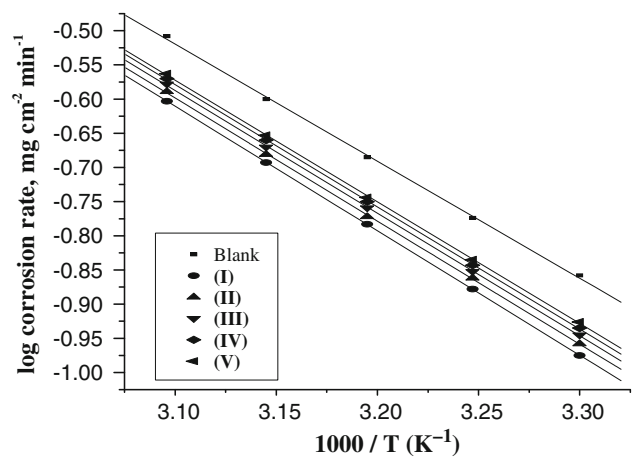

Fig. 3 Log corrosion rate (log k) vs. 1000/T for α-brass in the presence of 5×10^{-6} M inhibitors

concentration, the nature of the substituents, and their positions in the phenyl ring, with respect to the curcumin molecule derivatives. The curves obtained in the presence of inhibitors fall significantly below that of free acid. In all the cases, the increase in the inhibitor concentration was accompanied by a decrease in weight loss and an increase in the percentage inhibition. These results lead to the conclusion that these compounds under investigation are fairly efficient as inhibitors for α-brass dissolution in nitric acid solution. Also, the degree of surface coverage (θ) by the inhibitor, calculated from Eq 1, would increase by increasing the inhibitor concentration.

$$\Theta = [1 - (\Delta W_{\text{inh}}/\Delta W_{\text{free}})] \quad \text{(Eq 1)}$$

where ΔW_{inh} and ΔW_{free} are the weight losses per unit area in the presence and absence of the inhibitor, respectively.

In order to get a comparative view, the variation of the percentage inhibition (%IE) of the five inhibitors with their molar concentrations was calculated according to Eq 2. The values obtained are summarized in Table 1.

$$\%\text{IE} = \theta \times 100 \quad \text{(Eq 2)}$$

Careful inspection of these results showed that, at the same inhibitor concentration, the order of inhibition efficiencies is as follows: I > II > III > IV > V.

The variation of surface coverage determined by weight loss, θ, with the logarithm of the inhibitor concentration, log C, is represented in Fig. 2. These curves are of S-shape obeying the Frumkin adsorption isotherm (Ref 24) and are in good agreement with the Frumkin equation (Eq 3). From this figure, one can conclude that the degree of surface coverage increases as the concentration of the inhibitor increases and hence, the inhibition efficiency increases.

The Frumkin equation is

$$[\theta/1 - \theta]\exp(2\alpha\theta) = \text{KC} \quad \text{(Eq 3)}$$

where α is the molecular interaction parameter depending on the molecular interaction in the adsorption layer and on the degree of heterogeneity of the surface, C is the molar concentration of the inhibitor, and K is the equilibrium constant of the adsorption reaction.

3.1.1 Effect of Temperature. The effect of temperature on corrosion inhibition of α-brass in 2 M HNO_3 solution in the absence and presence of different concentrations of inhibitors (I-V) at different temperatures ranging from 30 to 50 °C was investigated. Arrhenius plot (Eq 4) of logarithm of the corrosion rate, log k, with the reciprocal of absolute temperature, 1/T, in the absence and presence of 5×10^{-6} M of inhibitors (I-V) is shown graphically in Fig. 3.

$$\text{In}k = B - \left(E_a^*/RT\right) \quad \text{(Eq 4)}$$

where B is the constant depending on the metal type and electrolyte, R is the universal gas constant, E_a* is the activation energy, and T is the absolute temperature. From the slopes of the plots, the respective activation energies (E_a*) were calculated and are tabulated in Table 2. Inhibitors may be classified into three groups according to the temperature effects (Ref 25):

(i) Inhibitors %IE of which decreases with increasing temperature. The value of E_a* is greater than that in the uninhibited solution;
(ii) inhibitors %IE of which does not change with increasing temperature. E_a* does not change with the presence or the absence of inhibitors; and
(iii) Inhibitors in the presence of which the %IE increases with increasing temperature, while the value of E_a* for corrosion process is smaller than that obtained in uninhibited solution.

The decrease in %IE with increasing temperature and higher value of the E_a* in presence of investigated compounds can be interpreted as an indication for physical or coulombic type of adsorption (Ref 26). The higher E_a* value in the inhibited solution can be correlated with the increased thickness of the double layer, which enhances the activation energy of the corrosion process. It is also indicated that the whole process is controlled by surface reaction, since the energy of the activation corrosion process is over 20 kJ/mol (Ref 27).

Enthalpy and entropy of activation (ΔH^*, ΔS^*) were calculated from the transition state theory (Ref 28) (Table 2):

$$k = (RT/Nh)\exp(\Delta S^*/R)\exp(-\Delta H^*/RT) \quad \text{(Eq 5)}$$

where h is the Planck's constant, and N is the Avogadro's number. A plot of log (k/T) vs. ($1/T$) (Eq 5) gave straight lines as shown in Fig. 4 for α-brass dissolution in 2 M HNO_3 in the absence and presence of 5×10^{-6} M of inhibitors (I). The positive signs of ΔH^* reflect the endothermic nature of α-brass dissolution process (Ref 29). The entropies of activation in the presence and absence of the inhibitors are large and negative. This implies that the activated complex in the rate-determining step represents association rather than dissociation, indicating that a decrease in disorder takes place on going from the reactant to the activated complex (Ref 30).

Table 2 Activation parameters for the dissolution of α-brass in 2 M HNO_3 in the absence and presence of 5×10^{-6} M of different inhibitors

Inhibitor	E_a*, kJ/mol	ΔH^*, kJ/mol	$-\Delta S^*$, J/mol·K
Blank	32.7	30.2	161.9
I	34.0	31.5	158.9
II	34.2	31.7	158.5
III	34.3	31.8	158.3
IV	34.4	31.9	158.1
V	34.8	32.3	157.2

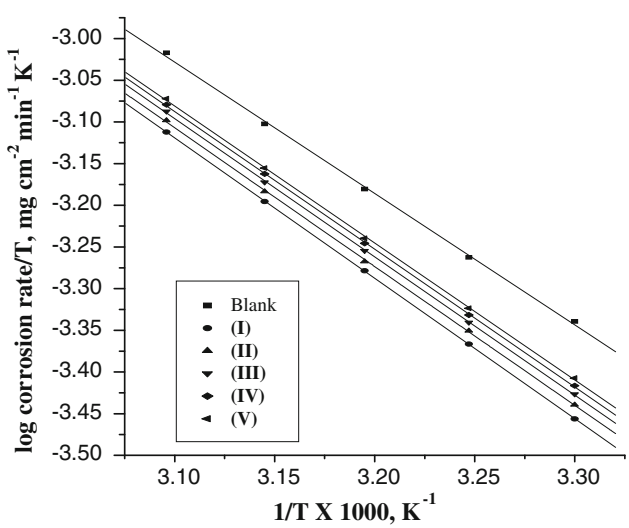

Fig. 4 Log k/T vs. $1/T$ for the corrosion rate of the α-brass in the presence of 5×10^{-6} M inhibitors

3.1.2 Synergistic Effect. The corrosion behavior of α-brass in 2 M nitric acid solution in the presence of 1×10^{-2} M potassium thiocyanate at different concentrations of inhibitors (I-V) was studied, and the calculated %IE values are summarized in Table 3. From these values, it is observed that %IE of the inhibitors increases in the presence of thiocyanate anions because of synergistic effects (Ref 31). The synergistic effect of this anion (SCN^-) has been observed by others (Ref 32). Adsorption of curcumin compounds at the α-brass/solution interface occurs through physical adsorption via electron-rich centers, i.e., benzene ring through its π-electrons, and nitrogen atom through their lone pairs of electrons by donation of electrons to the empty d-orbital of the metal (Ref 33). The synergistic inhibitive effect brought about by the concentrations of investigated compounds and thiocyanate anions on the corrosion of α-brass in 2 M HNO_3 can be explained as follows: The strong chemisorptions (Ref 34, 35) of (SCN^-) anions on the metal surface are responsible for the synergistic effect of the (SCN^-) anions with combination with the cationic forms of inhibitors. The inhibitors are then adsorbed by coulombic interaction on the metal surface where (SCN^-) anions are already adsorbed by chemisorptions. Stabilization of adsorbed thiocyanide anions with cations of inhibitors leads to greater surface coverage and therefore greater inhibition (Ref 36).

The synergism parameters (S_θ) were calculated using the relationship given by Aramaki et al. (Ref 37):

$$S_\theta = 1 - \theta_{1+2}/1 - \theta'_{1+2} \quad \text{(Eq 6)}$$

where $\theta_{1+2} = (\theta_1 + \theta_2) - (\theta_1\theta_2)$, θ_1 = surface coverage by anion, θ_2 = surface coverage by cation, and θ'_{1+2} is the measured surface coverage by both the anion and cation. S_θ approaches 1, when no interaction between the inhibitor compounds exists, while $S_\theta > 1$ points to a synergistic effect. In the case of $S_\theta < 1$, the antagonistic interaction prevails. Values of S_θ summarized in Table 4 are more than unity, suggesting that the phenomenon of synergism exists between the inhibitors and these additives.

Table 3 Inhibition efficiency of different inhibitors for α-brass in 2 M HNO_3 containing 1×10^{-2} M KSCN at 30 °C for an exposure period of 120 min

		% Inhibition efficiency				
Anion	Concentration, M	I	II	III	IV	V
KSCN	1×10^{-6}	77.7	76.7	75.9	75.0	74.1
	3×10^{-6}	80.1	78.4	77.3	76.5	75.7
	5×10^{-6}	82.4	80.4	79.2	78.8	77.1
	7×10^{-6}	84.4	82.9	80.9	80.4	78.4
	9×10^{-6}	86.3	85.2	82.7	82.0	80.0
	11×10^{-6}	88.3	86.7	84.3	83.5	81.6

Table 4 Synergism parameters (S_θ) for various concentrations of different curcumin compounds in the presence of 1×10^{-2} M KSCN

Anion	Concentration, M	% Inhibition efficiency				
		I	II	III	IV	V
KSCN	1×10^{-6}	0.832	1.031	1.008	0.998	0.986
	3×10^{-6}	1.117	1.046	1.009	0.995	0.973
	5×10^{-6}	1.169	1.090	1.058	1.021	1.006
	7×10^{-6}	1.245	1.138	1.103	1.063	1.014
	9×10^{-6}	1.310	1.128	1.129	1.095	1.018
	11×10^{-6}	1.463	1.182	1.224	1.146	1.033

Duration of the experiment: 120 min immersion

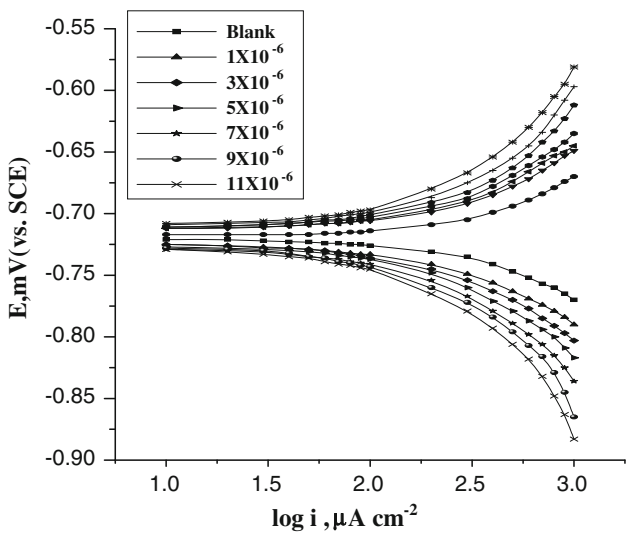

Fig. 5 Polarization curves for the dissolution of α-brass in 2 M HNO_3 in the presence and absence of different concentrations of compound I at 30 °C

3.2 Potentiodynamic Polarization Measurements

Figure 5 shows the potentiodynamic polarization curves for α-brass dissolution in 2 M HNO_3 in the absence and presence of different concentrations of inhibitor (I) at 30 °C. Similar curves were obtained for other inhibitors (not shown). The numerical values of the variation of the corrosion current density (i_{corr}), the corrosion potential (E_{corr}), Tafel slopes (b_a and b_c), the degree of surface coverage (θ), and the inhibition efficiency (%IE) with the concentrations of inhibitors (I-V) are given in Table 5.

The potentiodynamic curves show that there is a clear reduction of both anodic and cathodic currents in the presence of inhibitors compared to those for the blank solution. It is clear that the cathodic reduction (hydrogen evolution) and the anodic reaction (metal dissolution) were inhibited. The values of cathodic Tafel slope (b_c) for inhibitors are found to increase in the presence of inhibitors. The Tafel slope variation suggests that all inhibitors influence the kinetic of the hydrogen evolution reaction (Ref 38). This indicates an increase in the energy barrier for proton discharge, leading to less gas evolution (Ref 39). The approximately constant values of b_a for inhibitors indicate that these compounds were first adsorbed onto the brass surface and impeded by merely blocking the reaction sites of the brass surface without affecting the anodic reaction mechanism (Ref 40). The small changes in both b_a and b_c by adding inhibitors and the almost constant corrosion potential, E_{corr}, indicate that these compounds are of mixed-type. The orders of inhibition efficiency of all the inhibitors at different concentrations as given by polarization measurements are in good agreement with those obtained from weight-loss measurements.

3.3 Theoretical Studies

Quantum structure-activity relationships have been used to study the effect of molecular structure on %IE of the investigated inhibitors. Table 6 shows certain quantum-chemical parameters related to the molecular electronic structure, which were obtained by means of the application semi-empirical PM3 methods, such as (E_{HOMO}, E_{LUMO}) and the energy band gap ($\Delta E = E_{LUMO} - E_{HOMO}$), dipole moment (μ), and average of inhibition efficiencies (%IE). These parameters were calculated in liquid phase. The optimized structure and the highest occupied molecular orbital (HOMO) and the lowest unoccupied molecular orbital (LUMO) of inhibitors used are shown in Fig. 6. The HOMO energy (E_{HOMO}) is often associated with the electron-donating ability of the molecule. High (E_{HOMO}) values indicate that the molecule has a tendency to donate electrons to appropriate acceptor molecules with low energy empty molecular orbital. Increasing values of the E_{HOMO} facilitate adsorption (and therefore inhibition) by influencing the transport process through the adsorbed layer (Ref 41). E_{LUMO} indicates the ability of the molecules to accept electrons. The lower the values of the E_{LUMO}, the more the probability of the molecule accepting electrons (Ref 42, 43). Low absolute values of the energy band gap ($\Delta E = E_{LUMO} - E_{HOMO}$) will provide good inhibition efficiencies, because the energy to remove an electron from the last occupied orbital will be low (Ref 44).

From Table 6, it is evident that the values of the corrosion rate must decrease with increase in HOMO energy (less negative) for the studied compounds (Ref 45), and therefore, an increase in the corrosion inhibition is present. No relation was obtained between the inhibition efficiency (%IE) and the ionization potential of the inhibitor molecules. The results of this table show that the energies of the highest occupied molecular orbital (E_{HOMO}), values of E_{LUMO} and the energy gap (ΔE), decrease in the order: I > II > III > IV > V. This is in good agreement with the previously mentioned experimental data obtained by potentiodynamic polarization and weight loss techniques.

3.4 Chemical Structure and Corrosion Inhibition

Inhibition of the corrosion of α-brass in 2 M HNO_3 solution by some curcumin derivatives, determined by potentiodynamic polarization measurements, was found to depend on concentration, nature of metal, the mode of adsorption of the inhibitors, and surface conditions. These compounds can be adsorbed in a flat orientation through the oxygen of two (OH) groups/two (OCH_3) groups, and one (N) of the azo group. The surface coordination is through the nitrogen atoms. It was concluded that the mode of adsorption depends on the affinity of the metal toward the π-electron clouds of the ring system (Ref 40). Metals, such as Cu and Fe, which have a greater affinity toward aromatic moieties, were found to adsorb

Table 5 Electrochemical parameters for α-brass in 2 M HNO_3 with and without different concentrations of inhibitors at 30 °C

Inh.	Concentration, M	$-E_{corr}$, mV	i_{corr}, μA/cm^2	b_a, mV/dec	$-b_c$, mV/dec	θ	%IE
I	0.0	720	168.63	55	57	…	…
	1×10^{-6}	724	132.58	80	68	0.214	21.4
	3×10^{-6}	724	126.64	86	77	0.249	24.9
	5×10^{-6}	725	119.14	90	87	0.294	29.4
	7×10^{-6}	726	112.78	97	97	0.331	33.1
	9×10^{-6}	726	104.59	105	100	0.380	38.0
	11×10^{-6}	727	100.87	122	110	0.402	40.2
II	0.0	720	168.63	55	57	…	…
	1×10^{-6}	723	137.60	75	66	0.184	18.4
	3×10^{-6}	724	129.68	82	72	0.231	23.1
	5×10^{-6}	725	124.28	91	79	0.263	26.3
	7×10^{-6}	725	119.76	100	92	0.290	29.0
	9×10^{-6}	726	110.96	109	106	0.342	34.2
	11×10^{-6}	727	105.90	122	125	0.372	37.2
III	0.0	720	168.63	55	57	…	…
	1×10^{-6}	723	141.14	71	67	0.163	16.3
	3×10^{-6}	723	133.55	76	75	0.208	20.8
	5×10^{-6}	724	128.66	92	85	0.237	23.7
	7×10^{-6}	724	124.95	101	103	0.259	25.9
	9×10^{-6}	725	115.82	113	118	0.313	31.3
	11×10^{-6}	726	111.63	134	130	0.338	33.8
IV	0.0	720	168.63	55	57	…	…
	1×10^{-6}	723	142.49	62	58	0.155	15.5
	3×10^{-6}	723	136.25	71	71	0.192	19.2
	5×10^{-6}	724	131.70	83	83	0.219	21.9
	7×10^{-6}	725	125.97	102	104	0.253	25.3
	9×10^{-6}	726	118.55	123	118	0.297	29.7
	11×10^{-6}	726	113.39	139	133	0.328	32.8
V	0.0	720	168.63	55	57	…	…
	1×10^{-6}	722	147.72	59	57	0.124	12.4
	3×10^{-6}	723	138.11	67	66	0.181	18.1
	5×10^{-6}	723	134.40	84	80	0.203	20.3
	7×10^{-6}	724	128.66	103	108	0.237	23.7
	9×10^{-6}	724	119.89	124	126	0.289	28.9
	11×10^{-6}	725	112.64	153	147	0.311	31.1

Table 6 The calculated quantum chemical parameters of investigated compounds

Compound	E_{HOMO}, eV	E_{LUMO}, eV	ΔE, eV	μ, Debye
I	−9.069	−1.336	7.733	9.819
II	−9.090	−1.337	7.753	8.431
III	−9.091	−1.338	7.753	8.404
VI	−9.091	−1.342	7.749	8.445
V	−9.122	−1.367	7.755	14.327

benzene rings in a flat orientation. Thus, it is reasonable to assume that the tested inhibitors are adsorbed in a flat orientation through the N- and O-atoms. The order of decrease in the inhibition efficiency of the investigated inhibitors in the corrosive solution was as follows: I > II > III > IV > V.

This behavior can be rationalized on the basis of the structure-corrosion inhibition relationship of organic compounds. Linear free energy relationships (LFERs) have previously been used to correlate the inhibition efficiency of organic compounds with their Hammett constituent constants (σ) (Ref 42). The LFER or Hammett relations are given by (Ref 43-45).

$$\text{Log } k(\text{rate of corrosion}) = -\rho\sigma \quad \text{(Eq 6)}$$

where ρ is the reaction constant, and those constituents which attract electrons from the reaction center are assigned positive σ values and those which are electron donating have negative σ values. Thus, σ is a relative measure of the electron density at the reaction center. The slope of the plot of log (rate) vs. σ (Fig. 7) is ρ, and its sign indicates whether the process is inhibited by an increase or decrease of the electron density at the reaction center .The magnitude of ρ indicates the relative sensitivity of the inhibition process to electronic effects. The large positive slope of the correlation line (ρ = 0.994) shows a strong dependence of the adsorption character of the reaction center on the electron density of the ring. The strong dependence of the adsorption character of the reaction center on the electron density of the ring may be because, in this type of derivatives, the center of adsorption is conjugated to the ring.

Compound (I) has the highest percentage inhibition efficiency, this being due to the presence of *p*-OCH_3 group which is an electron repelling group with negative Hammett constant (σ = −0.27); this group will increase the electron charge density on the molecule. Compound (II) comes after compound

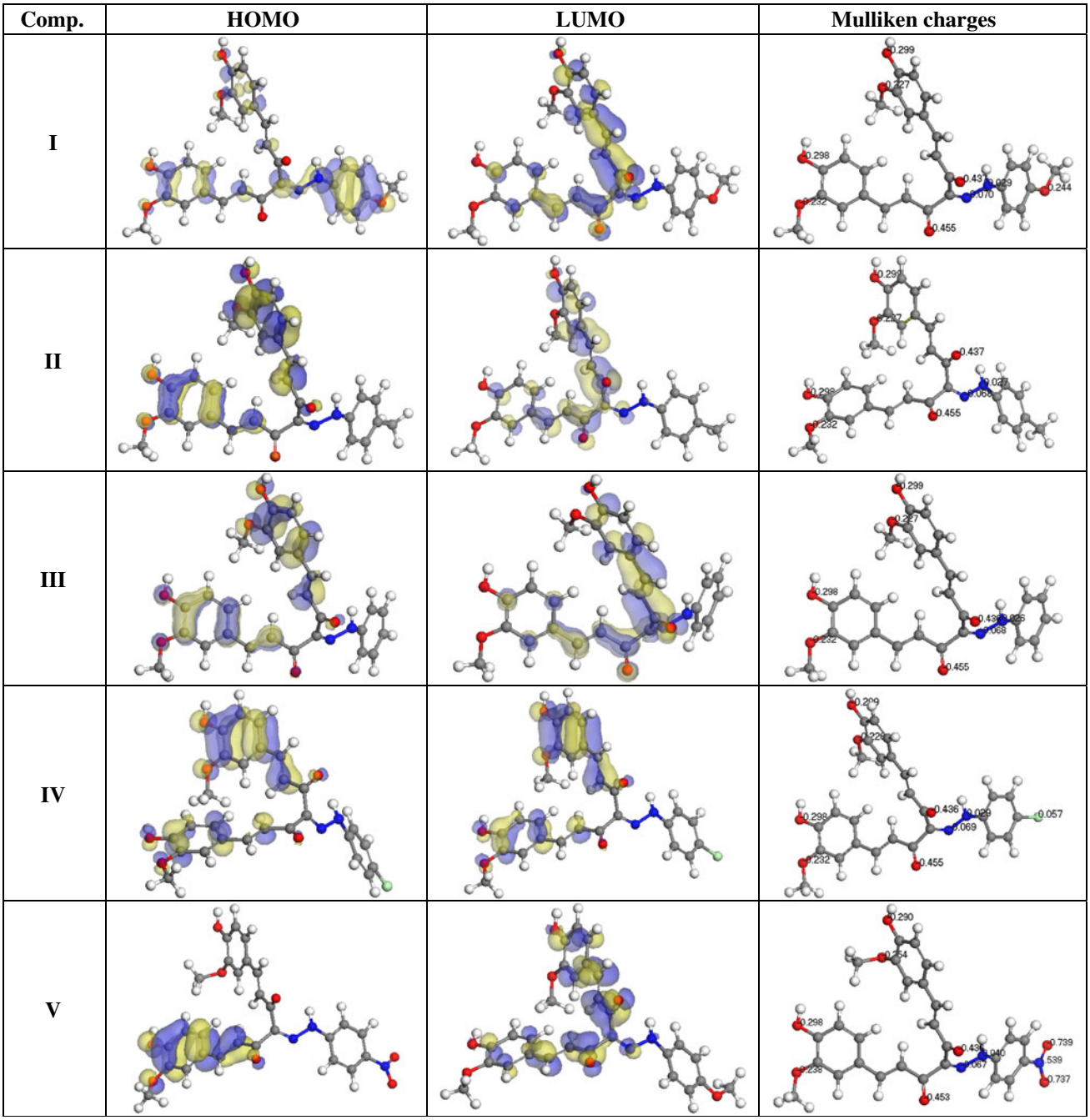

Fig. 6 Optimized molecular structures with Mulliken atomic charges of curcumin derivatives

(I); this is due to the presence of p-CH_3 group which is an electron-donating group with negative Hammett constant ($\sigma = -0.17$), Also this group will increase the electron charge density on the molecule but with lesser amount than p-OCH_3 group in compound (I). Compound (III) with Hammett constant ($\sigma = 0.0$) comes after compound (II) in percentage inhibition efficiency, because H-atom in p-position has no effect on the charge density on the molecules. Compound (IV) and (V) come after compound (III) in percentage inhibition efficiencies. This is due to both p-Cl and p-NO_2 groups being electron-withdrawing groups with positive Hammett constants ($\sigma_{Cl} = 0.23$, $\sigma_{NO_2} = 0.78$), and their order of inhibition depends on the magnitude of their withdrawing character.

4. Conclusions

The main conclusions are as follows:

1. Curcumin derivatives show good inhibitive action against the corrosion of α-brass in 2 M HNO_3.
2. The value of inhibition efficiency increases with increasing inhibitor concentration.
3. There is good agreement between the data obtained from weight loss and polarization methods.
4. The adsorption of curcumin derivatives on α-brass obeys Frumkin adsorption isotherm.

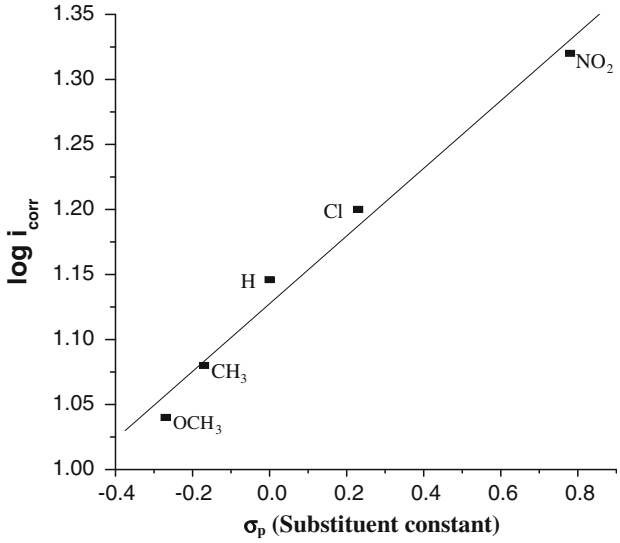

Fig. 7 Relation between log corrosion current density, log i_{corr} vs. Hammett constants, σ_p of the substituent from polarization measurements

5. The values of synergism parameters showed that inhibition of corrosion by curcumin derivatives and SCN^- ions was due to their co-adsorption.

References

1. S.L. Li, H.Y. Ma, S.B. Lei, R. Yu, S.H. Chen, and D.X. Liu, Inhibition of Copper Corrosion with Schiff Base Derived from 3-Methoxysalicylaldehyde and O-Phenyldiamine in Chloride Media, *Corrosion*, 1998, **54**, p 947–954
2. O.L. Riggs, *Theoretical Aspects of Corrosion Inhibitors and Inhibition*, NACE, Houston, TX, 1974
3. E.M. Sherif and S.M. Park, Effects of 2-Amino-5-Ethylthio-1,3,4-Thiadiazole on Copper Corrosion as a Corrosion Inhibitor in Aerated Acidic Pickling Solutions, *Electrochim. Acta*, 2006, **51**(28), p 6556–6562
4. E.M. Sherif, Effects of 2-Amino-5-(Ethylthio)-1,3,4-Thiadiazole on Copper Corrosion as a Corrosion Inhibitor in 3% NaCl Solutions, *Appl. Surf. Sci.*, 2006, **252**, p 8615–8623
5. F. Zucchi, G. Trabanelli, and M. Fonsati, Tetrazole Derivatives as Corrosion Inhibitors for Copper in Chloride Solutions, *Corros. Sci.*, 1996, **38**, p 2019–2029
6. E. Szocs, G. Vastag, A. Shaban, and E. Kalman, Electrochemical Behaviour of an Inhibitor Film Formed on Copper Surface, *Corros. Sci.*, 2005, **47**, p 893–908
7. J.C. Marconato, L.O. Bulhoes, and M.L. Temperini, A Spectroelectrochemical Study of the Inhibition of the Electrode Process on Copper by 2-Mercaptobenzothiazole in Ethanolic Solutions, *Electrochim. Acta*, 1998, **43**, p 771–780
8. R. Subramanian and V. Lakshminarayanan, Effect of Adsorption of Some Azoles on Copper Passivation in Alkaline Medium, *Corros. Sci.*, 2002, **44**, p 535–554
9. E.M. Sherif and S.-M. Park, Inhibition of Copper Corrosion in Acidic Pickling Solutions by *N*-phenyl-1,4-Phenylenediamine, *Electrochim. Acta*, 2006, **51**, p 4665–4673
10. E.M. Sherif and S.-M. Park, Inhibition of Copper Corrosion in 3.0% NaCl Solution by *N*-Phenyl-1,4-phenylenediamine, *J. Electrochem. Soc.*, 2005, **152**, p B428–B433
11. E. Stupnišek-Lisac, A. Brnada, and A.D. Mance, Secondary Amines as Copper Corrosion Inhibitors in Acid Media, *Corros. Sci.*, 2000, **42**, p 243–257
12. H. Ma, S. Chen, L. Niu, S. Zhao, S. Li, and D. Li, Inhibition of Copper Corrosion by Several Schiff Bases in Aerated Halide Solutions, *J. Appl. Electrochem.*, 2002, **32**, p 65–72
13. M. Ehteshamzadeh, T. Shahrabi, and M. Hosseini, 3,4-Dimethoxybenzaldehydethio-Semicarbazone as Corrosion Inhibitor, *Anti-Corros. Methods Mater.*, 2006, **53**(5), p 296–302
14. M. Ehteshamzadeh, T. Shahrabi, and M. Hosseini, Inhibition of Copper Corrosion by Self-Assembled Films of New Schiff Bases and Their Modification with Alkanethiols in Aqueous Medium, *Appl. Surf. Sci.*, 2006, **252**, p 2949–2959
15. A.A. El Warraky, The Effect of Sulphide Ions on the Corrosion Inhibition of Copper in Acidic Chloride Solutions, *Anti-Corros. Methods Mater.*, 2003, **50**(1), p 40–46
16. J.B. Matos, L.P. Pereira, S.M.L. Agostinho, O.E. Barcia, G.G.O. Cordeiro, and E. D'Elia, Effect of Cysteine on the Anodic Dissolution of Copper in Sulfuric Acid Medium, *J. Electroanal. Chem.*, 2004, **570**, p 91–94
17. G. Moretti and F. Guidi, Tryptophan as Copper Corrosion Inhibitor in 0.5 M Aerated Sulfuric Acid, *Corros. Sci.*, 2002, **44**, p 1995–2011
18. A.S. Fouda, A. Abd El-Aal, and A.B. Kandil, The Effect of Some Phthalimide Derivatives on the Corrosion Behaviour of Copper in Nitric Acid, *Anti-Corros. Methods Mater.*, 2005, **52**, p 96–101
19. G.K. Gomma and M.H. Wahdan, Temperature Coefficient of Corrosion Inhibition of Steel by Adenine, *Bull. Chem. Soc. Jpn.*, 1994, **67**, p 2621–2626
20. T. Choudhuri, S. Pal, T. Das, and G. Sa, Curcumin Induces Apoptosis in Human Breast Cancer Cells Through p53-Dependent Bax Induction, *FEBS Lett.*, 2002, **512**, p 334–340
21. R.K. Maheshwari, A.K. Singh, J. Gaddipati, and R.C. Srimal, Multiple Biological Activities of Curcumin: A Short Review, *Life Sci.*, 2006, **78**, p 2081–2087
22. A. Barik, B. Mishra, H. Mohan, S. Dutta, and H.-Y. Zhang, Evaluation of a New Copper(II)-Curcumin Complex as Superoxide Dismutase Mimic and Its Free Radical Reactions, *Free Radic. Biol. Med.*, 2005, **39**, p 811–822
23. A.A. Fadda, F.A. Badria, and K.M. El-Attar, Synthesis and Evaluation of Curcumin Analogues as Cytotoxic Agents, *Med. Chem. Res.*, 2010, **19**, p 413–430
24. N. Frumkin, Surface Tension Curves of the Higher Fatty Acids and the Equation of Condition of the Surface Layer, *J. Phys. Chem.*, 1925, **116**, p 466–484
25. O. Radovici, *Proceedings of the 2nd European Symposium on Corrosion Inhibitors* (Ferrara), 1965
26. K.K. Al-Neami, A.K. Mohamed, I.M. Kenawy, and A.S. Fouda, Inhibition of the Corrosion of Iron by Oxygen and Nitrogen Containing Compounds, *Monatsh. Chem.*, 1995, **126**, p 369–376
27. L. Larabi, O. Benali, S.M. Mekelleche, and Y. Harek, 2-Mercapto-1-methylimidazole as Corrosion Inhibitor for Copper in Hydrochloric Acid, *J. Appl. Surf. Sci.*, 2006, **253**, p 1371–1378
28. K. Haladky, L. Collow, and J. Dawson, Corrosion Rates from Impedance Measurements: An Introduction, *Br. Corros. J.*, 1980, **15**, p 20–25
29. M. Behpour, S.M. Ghoreishi, A. Gandomi-Niasar, N. Soltani, and M. Salavati-Niasari, The Inhibition of Mild Steel Corrosion in Hydrochloric Acid Media by Two Schiff Base Compounds, *J. Mater. Sci.*, 2009, **44**(10), p 2444–2453
30. M.A. Quraishi and S. Khan, Inhibition of Mild Steel Corrosion in Sulfuric Acid Solution by Thiadiazoles, *J. Appl. Electrochem.*, 2006, **36**, p 539–544
31. N. Cahskan and S. Bilgic, Effect of Iodide Ions on the Synergistic Inhibition of the Corrosion of Manganese-14 Steel in Acidic Media, *Appl. Surf. Sci.*, 2000, **153**, p 128–133
32. E. Khamis, E. El-Ashry, and A. Ibrahim, Synergistic Action of Vinyl Triphenyl Phosphonium Bromide with Various Anions on Corrosion of Steel, *Br. Corros. J.*, 2000, **35**, p 150–154
33. A. Yurt and Y. Mihrican, Quantitative Relationships Between the Structure of Some Thiol Compounds and Their Inhibition Efficiencies, *Anti-Corros. Methods Mater.*, 2008, **55**(4), p 195–203
34. I.A. Ammar, S. Darwish, and M. Etman, Adsorption of Iodide Ions on Polarized Iron, *Electrochim. Acta*, 1967, **12**, p 485–494
35. M. Jestonek and Z. Szklarska-Smialowska, The Inhibition of the Dissolution of Iron in Sulfuric Acid by Halide Ions, *Corros. Sci.*, 1983, **23**, p 183–187

36. E.E. Ebenso, Effect of Methyl Red and Halide Ions on the Corrosion of Aluminum in H_2SO_4 Center Dot Part 2, *Bull. Electrochem.*, 2004, **20**(12), p 551–559
37. K. Aramaki, M. Hagiwera, and H. Nishihara, The Synergistic Effect of Anions and the Ammonium Cation on the Inhibition of Iron Corrosion in Acid Solution, *Corros. Sci.*, 1987, **27**, p 487
38. G. Quartarone, L. Bonaldo, and C. Tortato, Inhibitive Action of Indole-5-Carboxylic Acid Towards Corrosion of Mild Steel in Deaerated 0.5 M Sulfuric Acid Solutions, *Appl. Surf. Sci.*, 2006, **252**, p 8251–8257
39. S.T. Selvi, V. Raman, and N. Rajendran, Corrosion Inhibition of Mild Steel by Benzotriazole Derivatives in Acidic Medium, *J. Appl. Electrochem.*, 2003, **33**, p 1175–1182
40. L.R. Chauhan and G. Gunasekaran, Corrosion Inhibition of Mild Steel by Plant Extract in Dilute HCl Medium, *Corros. Sci.*, 2007, **49**, p 1143–1161
41. M. Özcan, I. Dehri, and M. Erbil, Organic Sulphur-Containing Compounds as Corrosion Inhibitors for Mild Steel in Acidic Media: Correlation Between Inhibition Efficiency and Chemical Structure, *Appl. Surf. Sci.*, 2004, **236**, p 155–164
42. H. Ashassi-Sorkhabi, B. Shaabani, and D. Seifzadeh, Effect of Some Pyrimidinic Schiff Bases on the Corrosion of Mild Steel in Hydrochloric Acid Solution, *Electrochim. Acta*, 2005, **50**, p 3446–3452
43. H. Ashassi-Sorkhabi, B. Shaabani, and D. Seifzadeh, Corrosion Inhibition of Mild Steel by Some Schiff Base Compounds in Hydrochloric Acid, *Appl. Surf. Sci.*, 2005, **239**, p 154–164
44. G. Moretti, F. Guidi, and G. Grion, Tryptamine as a Green Iron Corrosion Inhibitor in 0.5 M Deaerated Sulphuric Acid, *Corros. Sci.*, 2004, **46**, p 387–403
45. V.S. Sastri and J.R. Perumareddi, Molecular Orbital Theoretical Studies of Some Organic Corrosion Inhibitors, *Corros. Sci.*, 1997, **53**, p 617–622